Check for updates

Synthesis and decarbonylation chemistry of gallium phosphaketenes†

Daniel W. N. Wilson,[a] William K. Myers [iD][b] and Jose M. Goicoechea [iD] *[a]

A series of gallium phosphaketenyl complexes supported by a 1,2-bis(aryl-imino)acenaphthene ligand (Dipp-Bian) are reported. Photolysis of one such species induced decarbonylation to afford a gallium substituted diphosphene. Addition of Lewis bases, specifically trimethylphosphine and the gallium carbenoid Ga(Nacnac) (Nacnac = HC[C(Me)N-(C_6H_3)-2,6-$^iPr_2$]$_2$), resulted in displacement of the phosphaketene carbonyl to yield base-stabilised phosphinidenes. In several of these transformations, the redox non-innocence of the Dipp-Bian ligand was found to give rise to radical intermediates and/or side-products.

The 2-phosphaethynolate anion (PCO⁻), a heavy analogue of cyanate (NCO⁻), is a useful precursor for the synthesis of phosphorus-containing heterocycles and low valent phosphorus compounds.[1] Access to such species typically involves salt metathesis reactions between [Na(dioxane)$_x$][PCO] and halogen-containing compounds, resulting in O- or P-substituted products. The latter coordination mode dominates the elements of the d- and p-block, allowing access to substituted phosphaketenes (E–P=C=O) which display a range of different reactivity modes. For the elements of the p-block a number of group 14 and 15 phosphaketene complexes have been reported to date.[2,3] By contrast, examples of group 13 phosphaethynolate complexes are still relatively rare. We previously reported on the synthesis of a phosphaethynolato-borane, [N(Dipp)CH]$_2$B(OCP) (Dipp = 2,6-diisopropylphenyl) (Fig. 1, **A**), and its subsequent isomerisation to yield its linkage isomer, [N(Dipp)CH]$_2$B(PCO) **B**, a phosphaketene.[4] We have since shown that these species can themselves act as synthons allowing access to a range of phosphorus containing molecules and metal complexes.[5] More recently, Grützmacher and co-workers reported the first examples of aluminium (**C**) and gallium (**D**) phosphaethynolate complexes stabilised by salen ligands.[6] The aluminium complex displays O-coordination whilst the gallium analogue was isolated as the P-bound isomer, in keeping with the decreasing oxophilicity upon descending the group, which in turn favours binding via

the phosphorus atom. The polydentate character of the salen ligand limits the further reactivity of these species, which behave indistinguishably from one another and in a comparable manner to ionic phosphaethynolate salts of the alkali and alkaline-earth elements.

Group 13 phosphaethynolate compounds are promising candidates as precursors to molecules and materials with interesting electronic properties. A recent study by Gilliard and co-workers showed that, upon photolysis, the boraphosphaketene, **E**, will decarbonylate affording a transient phosphinidene.[7] This highly reactive species inserts into a boron–aryl bond resulting in a BP-doped phenanthryne, the first example of such a species. In addition to giving rise to interesting molecular compounds, group 13 phosphaethynolates may provide new routes to group III/V semiconducting materials, which have desirable properties for use in photovoltaic devices, solid state lasers, LEDs, and optical waveguides.[8] A key limitation in understanding the potential of the group 13 phosphaethyno-
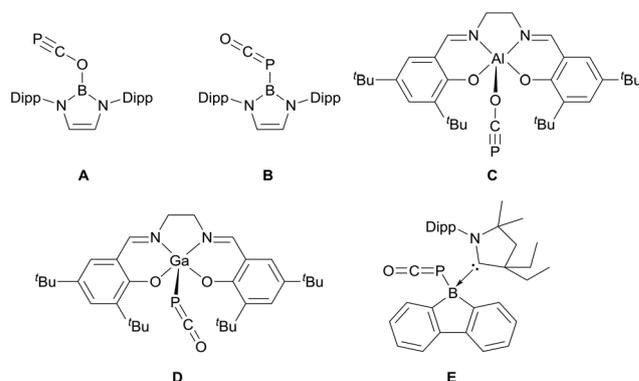
[a]Department of Chemistry, University of Oxford, Chemistry Research Laboratory, 12 Mansfield Road, Oxford, OX1 3TA, UK. E-mail: jose.goicoechea@chem.ox.ac.uk

[b]Department of Chemistry, University of Oxford, Centre for Advanced ESR, Inorganic Chemistry Laboratory, South Parks Road, Oxford, OX1 3QR, UK

†Electronic supplementary information (ESI) available: Full experimental details, NMR and EPR spectra, crystallographic data and computational results. CCDC 2025224–2025232. For ESI and crystallographic data in CIF or other electronic format see DOI: 10.1039/d0dt03174g

Fig. 1 Previously reported examples of group 13 phosphaethynolate compounds (Dipp = 2,6-diisopropylphenyl).
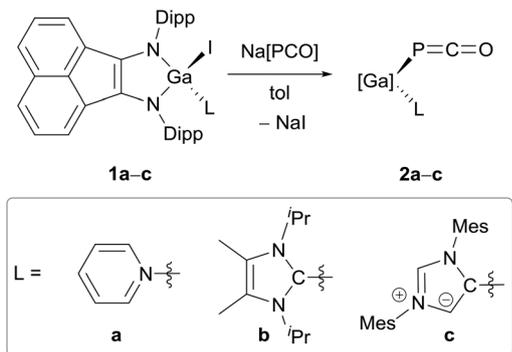
Scheme 1 Synthesis of phosphaketenes **2a–c**.

lates is their scarcity in the literature; the examples outlined in Fig. 1 represent the totality of structurally authenticated examples.

Given our previous success employing a bulky diamide ligand to stabilise phosphaethynolatoborane, **A**, we hypothesized that a similar ligand would be suitable for stabilising gallium phosphaethynolates. We selected the complex (Dipp-Bian)GaI(Pyr) (Dipp-Bian = 1,2-bis[(2,6-diisopropylphenyl)-imino]acenaphthene; Pyr = pyridine), (Scheme 1: **1a**), originally reported by Fedushkin and co-workers, for this purpose.[9] Modification of the literature procedure allowed for a one-pot synthesis of **1a** in good yields, bypassing several filtration and recrystallization steps, both of which can result in decomposition of this highly oxygen sensitive compound.‡ The pyridine ligand which occupies the fourth coordination site of the gallium centre can be displaced with N-heterocyclic carbenes (NHCs), namely 1,3-diisopropyl-4,5-dimethylimidazol-2-ylidene (^Me2^IPr) (**1b**) and 1,3-dimesitylimidazol-2-ylidene (IMes) (**1c**). These substitution reactions give access to a series of gallium iodide complexes with varied steric congestion about the gallium centre. It is noteworthy that in **1c** the IMes ligand adopts the abnormal coordination mode, resulting in a reduction in steric bulk with respect to **1b** and altering the electronic properties of the ligand.[10]

Reaction of **1a–c** with [Na(dioxane)$_{0.6}$][PCO] in toluene at room temperature results in conversion to the phosphaketenes **2a–c** as evidenced by singlet resonances in the ^{31}P{^{1}H} NMR spectra [δ = −394.6 (**2a**), −354.9 (**2b**), −374.2 ppm (**2c**)] and the characteristic phosphaketenyl carbon–phosphorus coupling in the ^{13}C NMR spectra [δ = 180.76 (d, $^1J_{P-C}$ = 101 Hz), 186.39 (d, $^1J_{P-C}$ = 85 Hz), 183.67 ppm (d, $^1J_{P-C}$ = 87 Hz) for **2a–c**, respectively]. These values are in good agreement to the previously reported salen-supported gallium phosphaketene [cf. ^{31}P{^{1}H} NMR δ = −376.9 ppm, ^{13}C NMR δ = 182.5 ($^1J_{P-C}$ = 88 Hz)].[6] In all cases, the ^{1}H NMR spectra are consistent with an asymmetric tetrahedral geometry at the gallium centre, evident from the presence of two isopropyl methine proton environments from the Dipp substituents. The preference for κ-P over

‡ See ESI† for full experimental details.

κ-O binding is in keeping with previous reports. No resonances corresponding to the phosphaethynolato species (*i.e.* [Ga]OCP) were observed upon formation of the phosphaketene. Crystals suitable for single-crystal X-ray diffraction studies were obtained by cooling saturated toluene (**2a** and **b**) or ether (**2c**) solutions for several days. The crystals exhibited pleochroism upon exposure to a polarised light source.

The solid-state structure of **2a** is shown in Fig. 2 (see ESI† for **2b–2c**). The bond angles about the phosphaethynolato moiety are typical of compounds of this class, with approximately linear O1–C1–P1 (177.2(11)–177.5(2)°) and Ga1–P1–C1 angles ranging from 85.6(1) to 91.0(5)°. Increasing the electron donating strength of the ligand (Pyr < ^Me2^IPr < ^ab^IMes) results in elongation of the C1–O1 bond with concurrent contraction of the C1–P1 bond, consistent with greater contribution from a resonance structure with increased C–P multiple-bond character. Whereas compound **2a** can be thought of as a covalently bonded gallium–phosphaketene, compounds **2b** and **2c** are more consistent with tight ion pairs between a cationic gallium complex and a phosphaethynolate anion. This is manifested in the Ga–P bond lengths (2.327(1) Å for **2a** and 2.430 (2)/2.411(3) for **2b/2c**, respectively).

In an effort to access terminal gallium phosphinidenes, [Ga]–P, toluene solutions of **2a–c** were irradiated at room temperature using a 600 W broadband UV lamp. In all cases, over time the ^{1}H and ^{31}P{^{1}H} NMR resonances corresponding to the phosphaketene diminish upon irradiation. In the case of **2a**, a small, broad resonance appears in the ^{31}P{^{1}H} spectrum at 774.9 ppm. Crystallisation of the reaction mixture allows for identification of this product as the diphosphene **3** (Scheme 2).

A related, boryl-substituted diphosphene was recently reported by our group under similar reaction conditions and displays a ^{31}P{^{1}H} NMR resonance at 596.2 ppm.[4b,11] The high
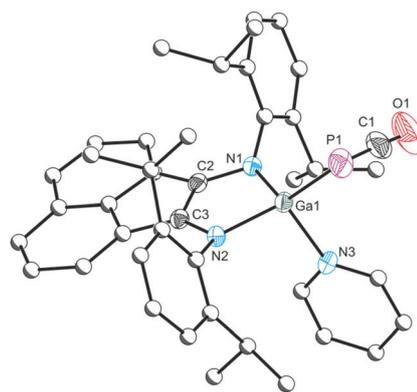

Fig. 2 Molecular structure of **2a**. Ellipsoids set at 50% probability; hydrogen atoms and solvent of crystallisation omitted for clarity. Carbon atoms of the Dipp, Bian and Pyr are pictured as spheres of arbitrary radius. Selected interatomic distances [Å] and angles [°]: Ga1–N1 1.892(1), Ga1–N2 1.906(1), Ga1–N3 2.056(1), Ga1–P1 2.327(1), P1–C1 1.636(3), C1–O1 1.165(3), N1–C2 1.397(2), N2–C3 1.399(2), N1–Ga1–N2 91.92(5), N1–Ga1–N3 101.91(5), N2–Ga1–N3 103.55(5), N1–Ga1–P1 125.96(4), N2–Ga1–P1 122.94(4), C1–P1–Ga1 85.61(7), O1–C1–P1 177.5(2).
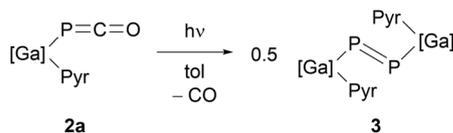
Scheme 2 Synthesis of diphosphene **3**.

frequency ^{31}P NMR shift observed for **3** is in keeping with studies by Niecke and co-workers. The greater degree to which the diphosphene substituent can act as a σ-donor and π-acceptor, the more deshielded the nucleus.[12] The solid-state structure displays a degree of coplanarity between the P_2 fragment and the Bian backbone (mean deviation from plane: 0.1761 Å) indicating back-donation from the phosphorus lone pairs into the vacant gallium p-orbitals. Density functional theory (DFT) calculations performed on **3** (PBE0/6-31 g(d,p)) are in good agreement with the observed $^{31}P\{^1H\}$ NMR resonance ($\delta_{calc} = 761$ ppm).

The solid-state structure of **3** contains an inversion centre at the P–P bond, resulting in equivalent bond metrics between the two halves of the molecule (Fig. 3). The P–P bond is in the expected range of a double bond (2.037(1) Å) and the Ga–P distance is consistent with a single bond (2.340(1) Å).[13] The Ga–P–P bond angle of 99.04(3)° is comparable to the aforementioned boryl-substituted diphosphene (*cf.* 97.02(4)°). Elemental analysis performed on the crystals is consistent with **3** being the sole product. Dissolving the crystals allowed for observation of the resonance at 774.9 ppm in the $^{31}P\{^1H\}$ NMR spectrum. However, the ^1H NMR spectrum displays broad resonances corresponding to the BIAN proton environments, preventing adequate assignment. Warming the solution above room temperature causes the irreversible disappearance of the $^{31}P\{^1H\}$ NMR resonance. In order to investigate the presence of paramagnetic species in solutions of **3**, EPR spectroscopy was performed. Solutions of the crystals gave rise to poorly resolved EPR signals, however confirmed the presence of a radical species. Monitoring the irradiation of **2a** allowed for observation of the same species over time, albeit with notably better spectral resolution. Unfortunately, how this species is related to **3** remains unclear, as we were unable to isolate this sample.

Irradiation of **2b** and **2c** resulted in no observable NMR resonances, including in the region corresponding to diphosphene **3**. The lack of observable diphosphene is likely a result of the increased steric requirement bestowed by the carbene ligands, inhibiting dimerisation. Reaction monitoring using EPR spectroscopy confirmed the presence of a radical species in both cases. It should be noted that **2a–c** all gave different signals, though **2b** and **2c** are visibly quite similar, implying the EPR signal is sensitive to substituents on the gallium centre. Attempts to crystallise these radical species frequently yielded yellow powders, likely to be the ligand, or bright green oils which were no longer soluble in common organic solvents. The prevalence of radical behaviour in these systems is unsurprising, as the Dipp-Bian ligand is non-innocent and has previously been employed to stabilise radicals in redox processes.[9,14] In this case, however, it is unclear what this process may be. Recent work by Power and co-workers investigated the nature of the tin–tin bond in ArSnSnAr (Ar = C_6H_3-2,6(C_6H_3-2,6-$^iPr_2$)$_2$), which undergoes reversible homolytic cleavage in solution to yield radical species as observed by EPR spectroscopy.[15] It could be proposed that upon irradiation of **2a**, yielding **3**, the steric bulk causes poor overlap of the P–P bonding orbitals resulting in heterolytic dissociation into radicals. Increasing the steric requirement at the gallium centre (**2b–c**) accelerates the dissociation into monomers, preventing the observation of the diphosphene by NMR spectroscopy. However, such a process has no precedent in the literature and, contrary to Power's ArSnSnAr system, we were unable to observe reformation of **3** upon cooling solutions of the radical species. Despite our best efforts, we were unable to unequivocally characterise the species present in solution on irradiation of **2a–c**.

We instead turned our attention to chemical decarbonylation processes. The substitution of the carbonyl ligand on phosphaketenes with stronger donors has previously been explored by the groups of Grützmacher and Bertrand utilising (phosphino)phosphaketenes, and by our group using a (boryl) phosphaketene.[3a,b,4b] Addition of trimethylphosphine to a toluene solution of **2a** (Scheme 3) resulted in quantitative formation of **4a**, as evidenced by the presence of a new AX spin system in the $^{31}P\{^1H\}$ NMR spectrum at 14.7 and −263.0 ppm
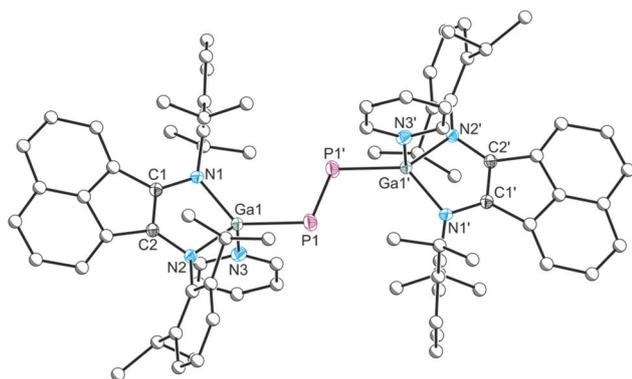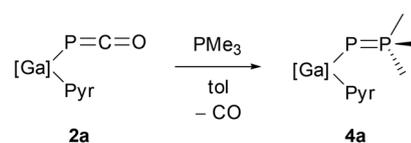

Fig. 3 Molecular structure of **3**. Ellipsoids set at 50% probability; hydrogen atoms and solvent of crystallisation omitted for clarity. Carbon atoms of the Dipp, Bian and Pyr are pictured as spheres of arbitrary radius. Selected interatomic distances [Å] and angles [°]: Ga−N1 1.904(2), Ga−N2 1.914(1), Ga−N3 2.079(2), Ga−P1 2.340(1), P1−P1 2.037(1), N1−C1 1.390(2), N2−C2 1.392(2), N1−Ga−N2 90.4(1), N1−Ga−N3 100.0(1), N2−Ga−N3 101.9(1), N1−Ga−P1 130.0(1), N2−Ga−P1 123.2(1), N3−Ga−P1 106.7(1), P1−P1−Ga 99.04(3).

Scheme 3 Ligand displacement to yield base stabilised phosphinidene **4a**.

Paper

(d, $^1J_{P–P}$ = 527 Hz). The ^1H NMR spectrum is consistent with higher order symmetry than the solid-state structure indicative of fluxional behaviour, which is rapid on the NMR timescale, likely caused by dissociation and reassociation of the pyridine ligand. The cause of this phenomenon may be due to an increase in availability of the phosphinidene lone pair to donate into the gallium p orbital, partially occupying the orbital and increasing the lability of the pyridine ligand. This manifests in a longer than expected Ga1–N3(pyr) bond length of 2.115(2) Å, Ga–N single bonds are typically expected around 1.95 Å (cf. 2.056(2) Å for **2a**). The increase in availability of the phosphinidene lone pair reflects the reduced π-acceptor ability of trimethylphosphine with respect to carbon monoxide, resulting in greater π-donation into the gallium p-orbital and a stronger Ga1–P1 bond.

The solid-state structure of **4a** (Fig. 4) reveals a short P1–P2 bond (2.084(2) Å), in line with what is expected of a double bond (2.04 Å) (Fig. 4).[13] This high bond order is also apparent from the large phosphorus–phosphorus coupling in the $^{31}P\{^1H\}$ NMR spectrum and can be rationalised through dative bonding from the trimethylphosphine to the phosphinidene accompanied by back donation from the phosphinidene lone pair into the phosphine σ* orbital. The Ga1–P1 bond length is 2.265(1) Å, slightly shorter than a typical single bond (Σ_{cov} = 2.35 Å).[13]

Addition of trimethylphosphine to **2b/c** results in no change to either the $^{31}P\{^1H\}$ or ^1H NMR spectra, consistent with both the increased steric protection given by the larger carbene ligands, and the stronger P–C bond as noted in solid state structure of **2b/c** compared to **2a**. Irradiation of these reaction mixtures results in silent NMR spectra. Crystals can be obtained from the irradiation of **2b** by cooling a concentrated toluene solution, allowing for identification of **4b**. This product confirms that irradiation is suitable for inducing dec-

arbonylation in the NHC substituted phosphaketene. Dissolving the crystals of **4b** yielded featureless NMR spectra, and EPR spectroscopy confirmed the presence of a radical species. Likewise, monitoring the irradiation of **2b** in the presence of PMe$_3$ using EPR spectroscopy allowed for observation of the radical species. Again, the identity of the species in solution is unknown.

The crystal structure of **4b** contains three crystallographically unique molecules; consequently, all bond distances are discussed as mean values. **4b** displays comparable bond metrics to **4a** with a P1–P2 bond of 2.083 Å and a Ga1–P1 bond of 2.319 Å.

After the initial success with phosphines, we sought to expand this methodology to allow access to phosphorus–heteroatom multiple bonds. We hypothesized that addition of Power's gallium(I) carbenoid Ga(Nacnac) (Nacnac = HC[C(Me)N-(C$_6$H$_3$)-2,6-^{i}Pr$_2$]$_2$) to the phosphaketene **2a** would result in decarbonylation.[16] The resulting compound would display a gallium–phosphorus bond with significant double bond character due to donation of the phosphinidene lone pair into the vacant p orbital of the gallium centre. We recently used this strategy to access a novel phosphanyl–phosphagallene (a species with a Ga=P double bond).[17]

Addition of a stoichiometric amount of Ga(Nacnac) to **2a** in toluene initially resulted in a mixture of two species as observed by $^{31}P\{^1H\}$ NMR spectroscopy, a singlet resonance at 157.3 ppm and a second singlet at −319.0 ppm. The former resonance can be tentatively assigned as the Ga(Nacnac) adduct **5I**. A similar species obtained from the reaction of a saturated phosphanyl phosphaketene with IDipp has previously been structurally authenticated.[18] This imidazolium adduct displays a $^{31}P\{^1H\}$ NMR resonances at 142.5 and 129.8 ppm (d, $^1J_{P–P}$ = 325.1 Hz), the former of these resonances corresponding to the relevant phosphorus atom. It was not possible to isolate **5I** as it slowly converts to the species at −319.0 ppm, identified as **5** (Scheme 4). Heating the solution to 70 °C expedites this process, resulting in complete consumption of **5I** in 30 minutes to yield **5** as the sole product.

Crystals of **5** were obtained by allowing a refluxing solution of toluene to cool slowly to room temperature. The solid-state structure reveals a bridging 2-coordinate phosphorus atom. The pyridine ligand has migrated to the less sterically congested Ga(Nacnac) centre, and the Ga2–N5 bond length is longer than a typical single bond (2.071(2) Å, Σ_{cov} = 1.95 Å) suggesting back donation from the phosphorus lone pair into
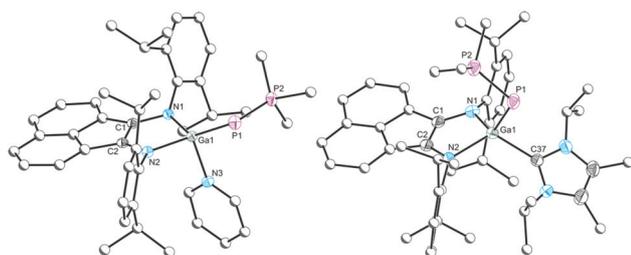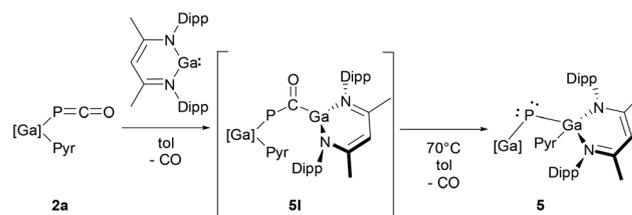

Fig. 4 Molecular structure of **4a** and **4b**. Ellipsoids set at 50% probability; hydrogen atoms and solvent of crystallisation omitted for clarity. Carbon atoms of the Dipp, Bian, Pyr, PMe$_3$ and ^{Me_2}IPr groups are pictured as spheres of arbitrary radius. Selected interatomic distances [Å] and angles [°]: **4a**; Ga1–N1 1.924(2), Ga1–N2 1.918(2), Ga1–N3 2.115(2), Ga1–P1 2.265(1), P1–P2 2.084(1), N1–C1 1.407(2), N2–C2 1.383(2), N2–Ga1–N1 90.7(1), N2–Ga1–N3 100.3(1), N1–Ga1–N3 96.7(1), N2–Ga1–P1 117.6(1), N1–Ga1–P1 137.2(1), N3–Ga1–P1 107.9(1), P2–P1–Ga1 100.9(1). **4b***; Ga1–N1 1.971, Ga1–N2 1.975, Ga1–C37 2.099, Ga1–P1 2.319, P1–P2 2.083, N1–Ga1–N2 87.9, N1–Ga1–C37 116.6, N2–Ga1–C37 120.29, N1–Ga1–P1 121.8, N2–Ga1–P1 121.3, C37–Ga1–P1 95.1, P2–P1–Ga1 103.7. *Given as mean values of three crystallographically unique molecules.

Scheme 4 Addition of Ga(Nacnac) to **2a** to yield **5**.

the gallium p-orbital. The Ga1–P1 and Ga2–P1 distances (2.207 (1) and 2.215(1) and Å, respectively) are intermediary between what is expected of single and double bonds (Σ_{cov} = 2.36 Å (single) and 2.19 Å (double)).[13] They are notably longer than reported examples of compounds containing a Ga=P bond (2.1650(7) and 2.1766(3) Å),[17] however a database search of structurally authenticated compounds with Ga–P bonds reveals that the bonds in **5** are the shortest unsupported Ga–P single bonds reported to date. The Ga1–P1–Ga2 bond is significantly bent, 112.7(1)°, contrary to what would be expected of a phosphaallene-type species with double bonds between the phosphorus and gallium atoms. Previously reported examples of bridging naked phosphorus atoms from the groups of Stephan and Cummins, in the complexes $(Cp_2Zr)_2(\mu\text{-}P)$ and $((Me_2N)_3Mo)(\mu\text{-}P)$, reveal linear bonding about the P centre.[19] The bond angle observed in **5** is comparable to that of a related bismuth and antimony radical species $[(Nacnac)GaI]_2Bi^\bullet$ and $[(Nacnac)GaCl]_2Sb^\bullet$ (*cf.* 106.68(3)° and 104.89(1)°), ruling out a description of two localised gallium phosphorus double bonds.[20]

The resonance structures of **5** with considerable weight are pictured in Fig. 6. This compound can be described as a zwitterion containing a monoanionic phosphorus atom with two lone pairs and two single bonds to each of the gallium metal centres (Fig. 6: **5i**). Alternatively, it can be described as a neutral species with a double bond between the phosphorus and the β-diketiminate gallium centre (**5ii**). Finally, moving the electron density to donate into the second Ga p-orbital results in a zwitterionic species with formal positive and negative charges on the two gallium centres (**5iii**). Carbene adducts of phosphinidenes have been established as indicators of the π-accepting properties of carbenes based on the shift of both the ^{13}C and ^{31}P NMR resonances, with increasing π-accepting carbenes shifting the phosphorus resonance to higher frequencies. Values previously reported for carbene adducts of an aryl-subtitutent phosphinidene range between −61.2 and 126.3 ppm (RPR′ where R = Ph and R′ = carbene), and a similar range was noted for carbene adducts of a (phosphanyl)phosphindene (−68 to +76 ppm).[21,22] Compound **5** is unusually situated in this series due to the relative electronegativity of gallium with respect to phosphorus, which results in an inversion of the polarity about the phosphinidene. The result is two σ-donating substituents with poor π-accepting properties and thus **5** exhibits a ^{31}P resonance at much lower frequency (−319.0 ppm) than related species.

To better understand the bonding situation in **5**, density functional theory (DFT) calculations were performed (PBE0/Def2TZVP (Ga, P, N)/Def2SVP (C, N)). The optimised structure, **5′**, displays bond parameters which are in good agreement with the solid-state data for **5**, displaying Ga1–P1 and Ga2–P1 bond lengths of 2.228 and 2.235 Å, respectively, and a Ga1–P1–Ga2 bond angle of 114.2°. Natural bond orbital analysis indicates the Ga1–P1 bond is slightly polarised towards the phosphorus (1.95e: 64.34% P; 35.66% Ga) and is comprised of primarily s orbital character from the gallium (76.30% s; 23.48% p) and p-orbital character from the phosphorus atom (14.41%

s; 84.67% p). Similarly, the interaction between Ga2 and P1 is again polarised towards the phosphorus centre (1.95e: 65.88% P; 34.12% Ga) with a similar orbital configuration of the bond (Ga2: 73.96% s; 18.87% p. P1: 18.87% s; 80.12% p). There are two lone pairs at the phosphorus centre, one with significant s-type character (1.82e: 65.21% s; 34.55% p) and one with almost entirely p-type character (1.74e: 1.33% s; 98.17% p). These lone pairs contribute to the HOMO and HOMO−1, respectively (Fig. 5). Natural population analysis indicates a significant negative charge localised on the phosphorus atom (*q* = −1.18) in comparison to Ga1 (*q* = +1.40) and Ga2 (*q* = +1.47). The short Ga1–P1 and Ga2–P1 interatomic distances can be attributed to attractive electrostatic interactions between the partially charged neighbouring atoms. **5** is best described as **5i** (Fig. 6), which bears an electronic resemblance to carbodiphosphoranes, carbon(0) compounds which are noted for their ability to act as double bases.[23,24] Studies into
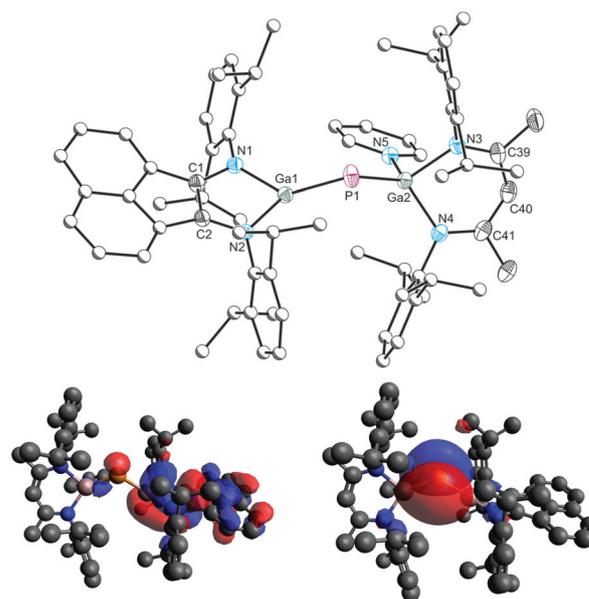

Fig. 5 Top: Molecular structure of **5**. Ellipsoids set at 50% probability; hydrogen atoms and solvent of crystallisation omitted for clarity. Carbon atoms of the Dipp, Bian and Pyr groups are pictured as spheres of arbitrary radius. Selected interatomic distances [Å] and angles [°]: Ga1−N1 1.911(2), Ga1−N2 1.889(1), Ga1−P1 2.207(1), Ga2−N3 1.965(2), Ga2−N4 1.965(2), Ga2−N5 2.071(2), Ga2−P1 2.215(1), N1−C1 1.392(3), N2−C2 1.383(3), N2−Ga1−N1 88.6(1), N2−Ga1−P1 122.6(1), N1−Ga1−P1 137.2(1), N3−Ga2−N4 94.8(1), N3−Ga2−N5 101.4(1), N4−Ga2−N5 100.0(1), N3−Ga2−P1 111.9(1), N4−Ga2−P1 127.7(1), N5−Ga2−P1 116.4(1), Ga1−P1−Ga2 112.7(1). Bottom: Kohn–Sham representation of the HOMO and HOMO−1 of **5′** (PBE0/Def2TZVP (Ga, P, N)/Def2SVP (C, N)).
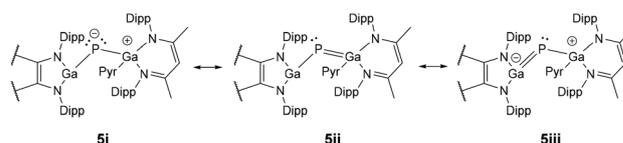

Fig. 6 Resonance structures of the phosphinidene adduct **5**.

the chemistry of **5** and its possible double-base character are ongoing.

In summary, we have isolated and characterised a series of gallium phosphaketenes obtained through salt metathesis between the corresponding gallium iodide and [Na(dioxane)$_x$][PCO]. The photolysis of phosphaketene **2a** results in decarbonylation to yield the first gallium-substituted diphosphene, **3**, which exhibits an unusually high frequency ^{31}P NMR resonance (δ = 774.9 ppm). Addition of trimethylphosphine to **2a** results in phosphine-stabilised phosphidene, **4a**, which displays a significant amount of negative hyperconjugation between the two phosphorus atoms, evidenced by a large phosphorus–phosphorus coupling constant ($^1J_{P-P}$ = 527 Hz) and a short interatomic distance in the solid state (2.084(2) Å). Similarly, addition of Power's gallium(I) carbenoid Ga(Nacnac) yields base-stabilised phosphinidene **5**. DFT investigation indicates **5** is best described as having two lone pairs at the phosphorus atom due to minimal electron donation to the adjacent gallium centres. As a result there is a significant negative charge localised at the phosphorus atom. This electronic situation resembles carbodiphosphoranes and may allow access to double-base reactivity of phosphorus.

Conflicts of interest

There are no conflicts to declare.

Acknowledgements

Notes and references

1 For recent reviews see: (*a*) L. Weber, *Eur. J. Inorg. Chem.*, 2018, **2018**, 2175–2227; (*b*) J. M. Goicoechea and H. Grützmacher, *Angew. Chem., Int. Ed.*, 2018, **57**, 16968–16994.

2 For examples of group 14 phosphaethynolates see: (*a*) D. Heift, Z. Benko and H. Grützmacher, *Dalton Trans.*, 2014, **43**, 5920–5928; (*b*) N. Del Rio, A. Baceiredo, N. Saffon-Merceron, D. Hashizume, D. Lutters, T. Müller and T. Kato, *Angew. Chem., Int. Ed.*, 2016, **55**, 4753–4758; (*c*) S. Yao, Y. Xiong, T. Szilvási, H. Grützmacher and M. Driess, *Angew. Chem., Int. Ed.*, 2016, **55**, 4781–4785; (*d*) Y. Wu, L. Liu, J. Su, J. Zhu, Z. Ji and Y. Zhao, *Organometallics*, 2016, **35**, 1593–1596; (*e*) Y. Xiong, S. Yao, T. Szilvási, E. Ballestero-Martínez, H. Grützmacher and M. Driess, *Angew. Chem., Int. Ed.*, 2017, **56**, 4333–4336.

3 For examples of group 15 phosphaethynolates see: (*a*) Z. Li, X. Chen, M. Bergeler, M. Reiher, C. Y. Su and H. Grützmacher, *Dalton Trans.*, 2015, **44**, 6431–6438; (*b*) L. Liu, D. A. Ruiz, D. Munz and G. Bertrand, *Chem*, 2016, **1**, 147–153; (*c*) M. M. Hansmann, D. A. Ruiz, L. Liu, R. Jazzar and G. Bertrand, *Chem. Sci.*, 2017, **8**, 3720–3725.

4 (*a*) D. W. N. Wilson, A. Hinz and J. M. Goicoechea, *Angew. Chem., Int. Ed.*, 2018, **57**, 2188–2193; (*b*) D. W. N. Wilson, M. P. Franco, W. K. Myers, J. E. McGrady and J. M. Goicoechea, *Chem. Sci.*, 2020, **11**, 862–869.

5 (*a*) D. W. N. Wilson and J. M. Goicoechea, *Chem. Commun.*, 2019, **55**, 6842–6845; (*b*) D. W. N. Wilson, N. H. Rees and J. M. Goicoechea, *Organometallics*, 2019, **38**, 4601–4606; (*c*) D. W. N. Wilson, M. Mehta, M. P. Franco, J. E. McGrady and J. M. Goicoechea, *Chem. – Eur. J.*, 2020, DOI: 10.1002/chem.202002226.

6 Y. Mei, J. E. Borger, D. J. Wu and H. Grützmacher, *Dalton Trans.*, 2019, **48**, 4370–4374.

7 W. Yang, K. E. Krantz, D. A. Dickie, A. Molino, D. J. D. Wilson and R. J. Gilliard, *Angew. Chem., Int. Ed.*, 2020, **59**, 3971–3975.

8 (*a*) F. Dimroth, *Phys. Status Solidi C*, 2006, **3**, 373–379; (*b*) H. Morkoç, S. Strite, G. B. Gao, M. E. Lin, B. Sverdlov and M. Burns, *J. Appl. Phys.*, 1994, **76**, 1363–1398; (*c*) K. J. Vahala, *Nature*, 2003, **424**, 839–846; (*d*) M. R. Krames, O. B. Shchekin, R. Mueller-Mach, G. O. Mueller, L. Zhou, G. Harbers and M. G. Craford, *J. Disp. Technol.*, 2007, **3**, 160–175; (*e*) R. J. Deri and E. Kapon, *IEEE J. Quantum Electron.*, 1991, **27**, 626–640.

9 I. L. Fedushkin, O. V. Kazarina, A. N. Lukoyanov, A. A. Skatova, N. L. Bazyakina, A. V. Cherkasov and E. Palamidis, *Organometallics*, 2015, **34**, 1498–1506.

10 For the chemistry of abnormal N-heterocyclic carbenes see: (*a*) R. H. Crabtree, *Coord. Chem. Rev.*, 2013, **257**, 755–766; (*b*) S. Sarmah, A. K. Guha and A. K. Phukan, *Eur. J. Inorg. Chem.*, 2013, **2013**, 3233–3239.

11 For a related boryl-substituted diphosphene see: S. Asami, M. Okamoto, K. Suzuki and M. Yamashita, *Angew. Chem., Int. Ed.*, 2016, **55**, 12827–12831.

12 (*a*) E. Niecke and D. Gudat, ^{31}P-NMR Spectroscopic Investigations of Low Coordinated Multiple Bonded PN-Systems, in *Phosphorus-31 NMR Spectral Properties in Compounds Characterization and Structural Analysis*, ed. L. Quin and J. G. Verkade, VCH Publishers, Deerfield Beach, 1994, pp. 159–174; (*b*) K. W. Zilm, G. G. Webb, A. H. Cowley, M. Pakulski and A. Orendt, *J. Am. Chem. Soc.*, 1988, **110**, 2032–2038.

13 (*a*) P. Pyykkö and M. Atsumi, *Chem. – Eur. J.*, 2009, **15**, 186–197; (*b*) P. Pyykkö and M. Atsumi, *Chem. – Eur. J.*, 2009, **15**, 12770–12779.

14 (*a*) H. Schumann, M. Hummert, A. N. Lukoyanov and I. L. Fedushkin, *Organometallics*, 2005, **24**, 3891–3896; (*b*) I. L. Fedushkin, A. A. Skatova, V. A. Dodonov, V. A. Chudakova, N. L. Bazyakina, A. V. Piskunov, S. V. Demeshko and G. K. Fukin, *Inorg. Chem.*, 2014, **53**, 5159–5170; (*c*) I. L. Fedushkin, O. V. Kazarina,

A. N. Lukoyanov, A. A. Skatova, N. L. Bazyakina, A. V. Cherkasov and E. Palamidis, *Organometallics*, 2015, **34**, 1498–1506; (*d*) I. L. Fedushkin, V. A. Dodonov, A. A. Skatova, V. G. Sokolov, A. V. Piskunov and G. K. Fukin, *Chem. – Eur. J.*, 2018, **24**, 1877–1889.

15 T. Y. Lai, L. Tao, R. D. Britt and P. P. Power, *J. Am. Chem. Soc.*, 2019, **141**, 12527–12530.

16 N. J. Hardman, B. E. Eichler and P. P. Power, *Chem. Commun.*, 2000, 1991–1992.

17 D. W. N. Wilson, J. Feld and J. M. Goicoechea, *Angew. Chem., Int. Ed.*, DOI: 10.1002/anie.202008207.

18 Z. Li, X. Chen, Z. Benkő, L. Liu, D. A. Ruiz, J. L. Peltier, G. Bertrand, C.-Y. Su and H. Grützmacher, *Angew. Chem., Int. Ed.*, 2016, **55**, 6018–6022.

19 (*a*) M. C. Fermin, J. Ho and D. W. Stephan, *Organometallics*, 1995, **14**, 4247–4256; (*b*) M. J. A. Johnson, P. Mae Lee, A. L. Odom, W. M. Davis and C. C. Cummins, *Angew. Chem., Int. Ed. Engl.*, 1997, **36**, 87–91.

20 C. Ganesamoorthy, C. Helling, C. Wölper, W. Frank, E. Bill, G. E. Cutsail and S. Schulz, *Nat. Commun.*, 2018, **9**, 1–8.

21 O. Back, M. Henry-Ellinger, C. D. Martin, D. Martin and G. Bertrand, *Angew. Chem., Int. Ed.*, 2013, **52**, 2939–2943.

22 M. M. Hansmann, R. Jazzar and G. Bertrand, *J. Am. Chem. Soc.*, 2016, **138**, 8356–8359.

23 (*a*) F. Ramirez, N. B. Desai, B. Hansen and N. McKelvie, *J. Am. Chem. Soc.*, 1961, **83**, 3539–3540; (*b*) G. E. Hardy, J. I. Zink, W. C. Kaska and J. C. Baldwin, *J. Am. Chem. Soc.*, 1978, **100**, 8002–8002; (*c*) R. Tonner, F. Öxler, B. Neumüller, W. Petz and G. Frenking, *Angew. Chem., Int. Ed.*, 2006, **45**, 8038–8042.

24 A comparison can also be drawn with mono-cationic base-stabilised nitrogen (+1) compounds, so-called "nitreones". For representative examples see: (*a*) R. A. Kunetskiy, I. Císařová, D. Šaman and I. M. Lyapkalo, *Chem. – Eur. J.*, 2009, **15**, 9477–9485; (*b*) T. Ma, X. Fu, C. W. Kee, L. Zong, Y. Pan, K.-W. Huang and C.-H. Tan, *J. Am. Chem. Soc.*, 2011, **133**, 2828–2831; (*c*) P. V. Bharatam, M. Arfeen, N. Patel, P. Jain, S. Bhatia, A. K. Chakraborti, S. Khullar, V. Gupta and S. K. Mandal, *Chem. – Eur. J.*, 2016, **22**, 1088–1096; (*d*) T. Singh and P. V. Bharatam, *J. Comput. Chem.*, 2019, **40**, 2207, and references therein.